Vol. 604: 65–81, 2018
https://doi.org/10.3354/meps12721

MARINE ECOLOGY PROGRESS SERIES
Mar Ecol Prog Ser

Published October 4

Primary production and community structure of coastal phytoplankton in the Adriatic Sea: insights on taxon-specific productivity

Iva Talaber[1,2,*], Janja Francé[1], Vesna Flander-Putrle[1], Patricija Mozetič[1]

[1]National Institute of Biology, Marine Biology Station Piran, Fornače 41, 6330 Piran, Slovenia
[2]University of Ljubljana, Biotechnical faculty, Večna pot 111, 1000 Ljubljana, Slovenia

ABSTRACT: We examined the relationship between phytoplankton primary production, biomass and community structure in a 2-year *in situ* survey in a predominantly bottom-up limited coastal sea (Gulf of Trieste, Adriatic Sea). Our results suggest that nutrient supply primarily shapes the phytoplankton community structure, which in turn governs the magnitude of primary production through the relative contribution of different phytoplankton groups and their group-specific chl *a*-normalized primary production. Non-metric multidimensional scaling analysis with superposed thin plate regression splines was used to relate chl *a*-normalized primary production with each phytoplankton group, of which cyanobacteria were associated with the highest and diatoms with the lowest chl *a*-normalized primary production (>5 and 1–2 mg C [mg chl *a*]$^{-1}$ h^{-1}, respectively). However, both groups were associated with periods of high primary production, highlighting the taxonomic differences in phytoplankton functional traits. Annual primary production for the years 2010 and 2011, characterized by different nutrient availability especially during summer, was estimated at 87.4 and 60.2 g C m^{-2}, respectively. Hence, even short-lived freshwater pulses during the annual irradiance maximum, sustaining a diatom-dominated assemblage rich in biomass, can substantially increase the annual primary production.

KEY WORDS: Phytoplankton · Photosynthetic pigments · Primary production · Chl *a*-normalized primary production · Nutrients · Coastal sea

INTRODUCTION

In coastal seas, characterized by the dominant influence of river input, the potential for phytoplankton primary production (PP) is set by the nutrient supply rate (Howarth 1988). The realization of that potential is in turn determined by the balance between growth, mortality and transport of phytoplankton biomass (Cloern et al. 2014). Nevertheless, for globally representative data sets, phytoplankton biomass alone (represented by the concentration of chlorophyll *a* [chl *a*]) accounts for up to 40% of the variability in PP (Behrenfeld et al. 2002) and as much as 85% of the variability in coastal and estuarine environments (Cole & Cloern 1984, Keller et al. 2001, Murrell et al. 2007). However, variability in phytoplankton photophysiology confounds this relationship (Bouman et al. 2010, Gallegos 2014) and the inclusion of the water column maximum chl *a*-normalized carbon fixation rate (P^B_{opt}; see 'Materials and methods: *In situ* PP' for definition) can significantly improve model estimates of water column integrated PP (Behrenfeld & Falkowski 1997). The consideration of P^B_{opt} is even more critical in oligotrophic environments, where the chl *a* concentration is highly constrained (Banse & Yong 1990, Behrenfeld et al. 2002). Furthermore, as phytoplankton photophysiology seems to be taxon- and/or size-specific (Claustre

*Corresponding author: iva.talaber@gmail.com

et al. 2005, Uitz et al. 2008, Richardson et al. 2016), the role of phytoplankton community structure should ideally be included in PP studies. Instead of relating photosynthetic performance solely to environmental variables, an increasing number of studies is highlighting the need to focus PP research on the relationship between the abiotic environment, phytoplankton community structure and photophysiology (Bouman et al. 2003, Uitz et al. 2010 and references therein, Richardson et al. 2016). To achieve this, long term PP measurements and phytoplankton community sampling *in situ* are most appropriate, especially in coastal environments, where suspended sediments, dissolved organic matter, and interference from land can confound the interpretation of ocean color (Moreno-Madriñán & Fischer 2013). While recent technological progress has resulted in a more accurate satellite retrieval of phytoplankton biomass (Blondeau-Patissier et al. 2014), the remote sensing of phytoplankton community structure is still limited (Bracher et al. 2017).

The Gulf of Trieste is part of the northern Adriatic, which has experienced a eutrophication trend (Revelante & Gilmartin 1983, Pugnetti et al. 2005) in the last 3 decades of the 20th century, due to substantial inputs of nitrogen and phosphorus delivered by the Po River (Degobbis & Gilmartin 1990). However, a reversal in the eutrophication trend occurred during early 2000s (Mozeti et al. 2010, Giani et al. 2012 and references therein), which, in addition to scarce measurements of PP in the Gulf of Trieste (Cantoni et al. 2003, Fonda Umani et al. 2007, Cibic et al. 2018), necessitates a re-evaluation of primary production in this area. Importantly, the trophic shift resulted in an increasing abundance of nanoflagellates at the expense of diatoms (Mozeti et al. 2012) on an annual scale, which highlights the role of potential taxonomic differences in photophysiology for the annual PP in this ecosystem.

We present a comprehensive 2-year data set of temporally and vertically resolved PP measurements *in situ*, coupled with data on phytoplankton community structure, inferred from high-performance liquid chromatography (HPLC) biomarker pigment analysis. The aim of this study was to examine the relationship between PP, chl *a* and community structure in natural populations of phytoplankton on an annual scale. Aside from estimating daily and annual rates of PP, which are of great local relevance, we relate PP of phytoplankton to its community structure and the photophysiological parameter P^B_{opt}, which is equally relevant for other coastal areas with similar phytoplankton community patterns. An additional aim was to determine the vertical profile of PP and its contribution to the vertically integrated PP, as the shallow and euphotic water column in the Gulf of Trieste is generally stratified (Talaber et al. 2014), possibly enabling vertical heterogeneity in phytoplankton biomass and community structure.

MATERIALS AND METHODS

Study site

The Gulf of Trieste is a shallow basin at the northernmost end of the Adriatic Sea (Fig. 1), with a maximal depth of 25 m. Its hydrology is heavily influenced by river inputs, especially from the largest rivers, Po and Soča (Isonzo), and by water mass exchange with the northern Adriatic at the

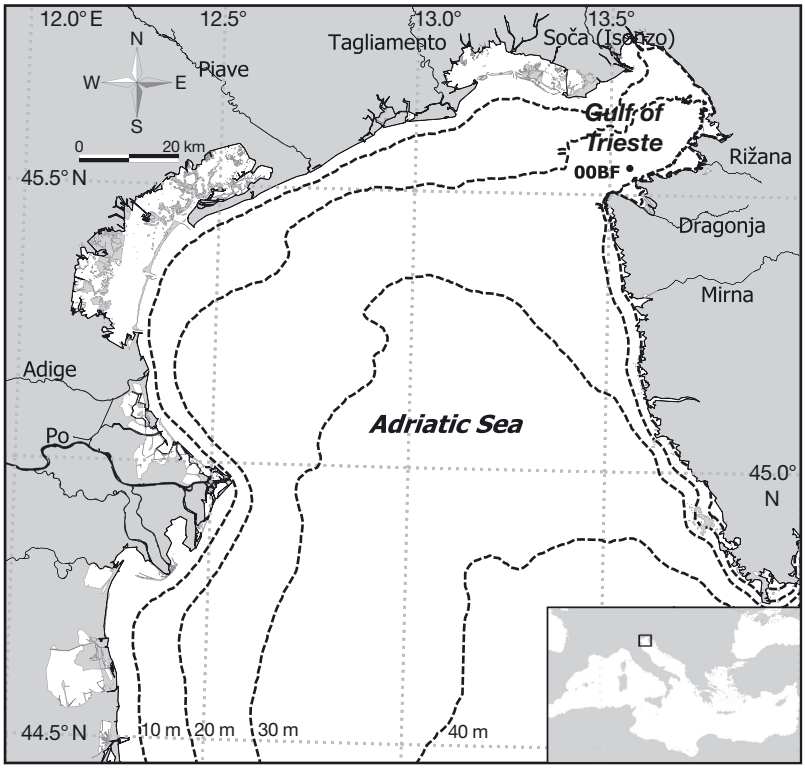

Fig. 1. Sampling station (00BF) in the Gulf of Trieste. Inset: the Adriatic Sea and the Mediterranean

open boundary (Malačič et al. 2006). Nutrient supply is driven by local river run-offs (Cozzi et al. 2012), which depend on the regional meteorological pattern (Comici & Bussani 2007). Phytoplankton dynamics in the Gulf of Trieste are predominantly controlled by bottom-up process (Mozetič et al. 2012).

Sampling and analyses

Sampling was carried out biweekly during the period 2010–2011, at an offshore station (1.3 nautical miles off the coast, depth of 22 m) in the south-eastern part of the Gulf of Trieste (station 00BF, Fig. 1).

Standard vertical profiles included measurements of temperature, salinity, density (σ_T), and photosynthetically available radiation (PAR), using the fine-scale CTD probe (Sea & Sun Technology), with a LI-192SA Underwater Quantum sensor (LI-COR). From the vertical profiles of PAR, we extracted the irradiance at depth z (E_z) and at 0.3 m below the sea surface (E_{surf}). The attenuation coefficient (K_d) was derived from the PAR profiles for each sampling. It was determined as the slope of the natural logarithm of the downwelling PAR (E_z) plotted with depth, assuming exponential attenuation according to the Lambert-Beer law (Kirk 1994), given in equation (1).

$$E_z = E_{surf} \times \exp(K_d \times z) \quad (1)$$

Optical depths (ζ) were calculated as:

$$\zeta = -z \times K_d \quad (2)$$

Water samples for nutrients, chl *a*, biomarker pigments and PP analysis were collected at 5 depths: 0, 5, 10, 15 and 21 m with a SBE 32 Carousel water sampler (Sea-Bird Scientific) equipped with 5 l Niskin bottles. Concentrations of inorganic nutrients (nitrate, ammonium, phosphate and silicate) were measured on unfiltered samples following standard colorimetric methods (Grasshoff et al. 1983) and their modifications (Grasshoff et al. 1999).

The photosynthetic pigments, chl *a* included, were determined using a reverse-phase HPLC method (Mantoura & Llewellyn 1983, Barlow et al. 1993). Water samples (1 l) were filtered through 47 mm Whatman GF/F filters and immediately frozen until analyzed (at −80°C). Frozen samples were extracted in 4 ml of 90% acetone, using sonication, and centrifuged 10 min at 2600 × *g* to remove particles. Mixture (1:1) of clarified extract and 1 mol l^{-1} ammonium acetate was injected into a gradient HPLC system (1260 Infinity, Agilent Technologies) with a 200 µl loop. The HPLC system was equipped with a reverse-phase 3 µm C18 column (Pecosphere, 35 × 4.5 mm, Perkin Elmer). Chlorophylls and carotenoids were detected by absorbance at 440 nm using a diode-array detector (1290 Infinity, Agilent Technologies). Data collection and integration were performed with Agilent ChemStation software. To estimate the contribution of various phytoplankton groups, we multiplied the concentrations of individual biomarker pigments with published values of chl-*a*:biomarker-pigment ratios (*K*; Table 1). The contribution of different phytoplankton groups to total chl *a* was estimated using the equation:

$$X = K\,[C_{pig}\,(C_{chl\ a})^{-1}] \quad (3)$$

where X is the phytoplankton group specific percentage of chl *a*, K is the chl-*a*:biomarker-pigment ratio for a specific phytoplankton group, C_{Pig} is the concentration of biomarker pigment for that phytoplankton group, and $C_{chl\ a}$ is the concentration of chl *a* in the sample.

In situ PP

Three subsamples from each sampled depth were inoculated with 185 kBq $NaH^{14}CO_3$ in 75 ml polycarbonate bottles (2 light and 1 dark) and incubated from 10:00 to 14:00 h (t_{inc} = 4 h) at their respective *in situ* depth. After incubation subsamples were filtered on 25 mm Whatman GF/F filters. The filters were acidified with 250 µl of 0.1 M HCl overnight to eliminate any unfixed carbon. After adding 10 ml of Ultima Gold (Sigma-Aldrich) scintillation cocktail, the activity of the samples was determined in a TriCarb 3100TR liquid scintillator (Perkin-Elmer).

Table 1. Values of chl-*a*:biomarker-pigment ratios (*K*) in different phytoplankton groups and their biomarker pigments

Phytoplankton group	Biomarker pigment	*K*	Reference
Diatoms	Fucoxanthin	1.2	Terzić (1996)
Prymnesiophytes	19′-hexanoyloxyfucoxanthin	1.1	Terzić (1996)
Dinoflagellates	Peridinin	1.5	Terzić (1996)
Cyanobacteria	Zeaxanthin+lutein	1.7	Stransky & Hager (1970)
Silicoflagellates	19′-butanoyloxyfucoxanthin	1.6	Everitt et al. (1990)
Cryptophytes	Alloxanthin	1.85	Hager & Stransky (1970)
Chlorophytes	Chlorophyll *b*	0.9	Terzić (1996)

Hourly rates of net PP were calculated as described by Gargas (1975) for each sampling depth:

$$PP = (A_1 \times [CO_2] \times 12 \times 1.05 \times 1.06) / (A_2 \times t \times 1000) \quad (4)$$

where A_1 is the activity of the sample ($dpm_{(light)} - dpm_{(dark)}$), with $dpm_{(light)}$ being the average of the 2 light bottles, A_2 is the activity of the added isotope, $[CO_2]$ is the concentration of CO_2 (mM) calculated from temperature, salinity and pH (Strickland & Parsons 1968), 12 is the atomic mass of carbon and t is the length of incubation. The multiplication factor 1.05 accounts for the preferential uptake of ^{12}C over ^{14}C, 1.06 corrects for autotrophic respiration and multiplying by 1000 accounts for converting mg l^{-1} to mg m^{-3}.

The maximal value of PP of all 5 sampling depths was designated as P_{opt}, which is the maximum PP of the water column. Normalizing P_{opt} to chl *a* at its respective depth (chl a_{opt}) yields P^B_{opt}, which is the maximum chl *a*-normalized PP of the water column.

To estimate the hourly (mg C m^{-2} h^{-1}) and annual (g C m^{-2} yr^{-1}) integrated PP (INT PP) as well as the water column integrated concentration of chl *a* (INT chl *a*; mg m^{-2}), we calculated the contribution of each sampling depth with the trapezoidal rule.

To calculate daily integrated PP (mg C m^{-2} d^{-1}) we multiplied the hourly value with the unitless daylight factor D, to account for the difference between the number of hours during incubation (t_{inc} = 4) and the number of hours of daylight

$$D = (\sum E_{0(24h)} / \sum E_{0(inc)}) \times t_{inc} \quad (5)$$

where $E_{0(24h)}$ is the cumulative incident light during 24 h and $E_{0(inc)}$ is the cumulative surface irradiance during incubation. Incident light (E_0) was measured with a PAR sensor (LI-190SA Quantum sensor), attached to the roof of the research vessel.

Statistical analyses

The distribution of data was generally not normal according to the Kolmogorov-Smirnov test (Dytham 2011). The relationship between abiotic and biotic parameters was therefore evaluated with the Spearman's rank correlation, which does not require any assumptions about distribution (Iman & Conover 1982). Patterns of the temporal distribution of the phytoplankton community in terms of relative contribution of phytoplankton groups to total biomass (group specific percentage of chl *a*) were explored by non-metric multidimensional scaling analysis (nMDS; Legendre & Legendre 2012). The ordination was based on Bray-Curtis distance matrix. Abiotic parameters were subsequently fitted to the ordination with the *envfit* function in R (R Development Core Team 2012), to indicate their relation to phytoplankton community structure. To get the visual representation of the distribution of P_{opt}, P^B_{opt} and chl *a* in association with the phytoplankton community structure in the surface (1 and 5 m), their values were projected as contours on the ordination space using thin plate regression splines (TPS; Wood 2003). The nMDS and TPS analyses were made in the free software R version 2.15.0. To increase the statistical sample size of the surface phytoplankton sample for the analysis of relationship between environmental factors, phytoplankton production and community structure, we treated both PP_{1m} and PP_{5m} as P_{opt}, as PP was very similar at 1 and 5 m (<25% difference) in almost all cases. Exceptions were only made for the 2 August 2011 samples, where PP was considerably lower at 1 m compared to 5 m (>25% difference) and only the higher value was treated as P_{opt}. In the one case, where P_{opt} occurred at 15 m (26 August 2010), we used the surface value instead, because the accompanying abiotic parameters of the true P_{opt} value were statistical outliers.

RESULTS

Physical and chemical properties of the water column

Abiotic parameters showed a typical seasonal dynamic, with a temperature peak in summer and a salinity peak in winter (Fig. 2). Aside from the winter period, when the euphotic zone could be shallower than the water column depth, light intensity within the first optical depth (~within the first 5 m) was generally >750 µmol photons m^{-2} s^{-1} and between 0 and 1000 µmol photons m^{-2} s^{-1} in the deeper half of the water column. (Fig. 2a). Nutrient concentration varied considerably over the studied period. Nitrate surface peaks were in the spring period of both years (April–June 2010, April and June 2011), coinciding with drops in surface salinity (Fig. 2c). Higher nitrate concentrations along the whole water column occurred in late autumn and winter (November 2010–January 2011, October and December 2011) (Fig. 2e). The autumn peak of 2010 (17.54 µM) was about 4 times higher than that of 2011 (4.62 µM). In contrast to nitrate, phosphate and ammonium peaks were found deeper in the water column, frequently at the

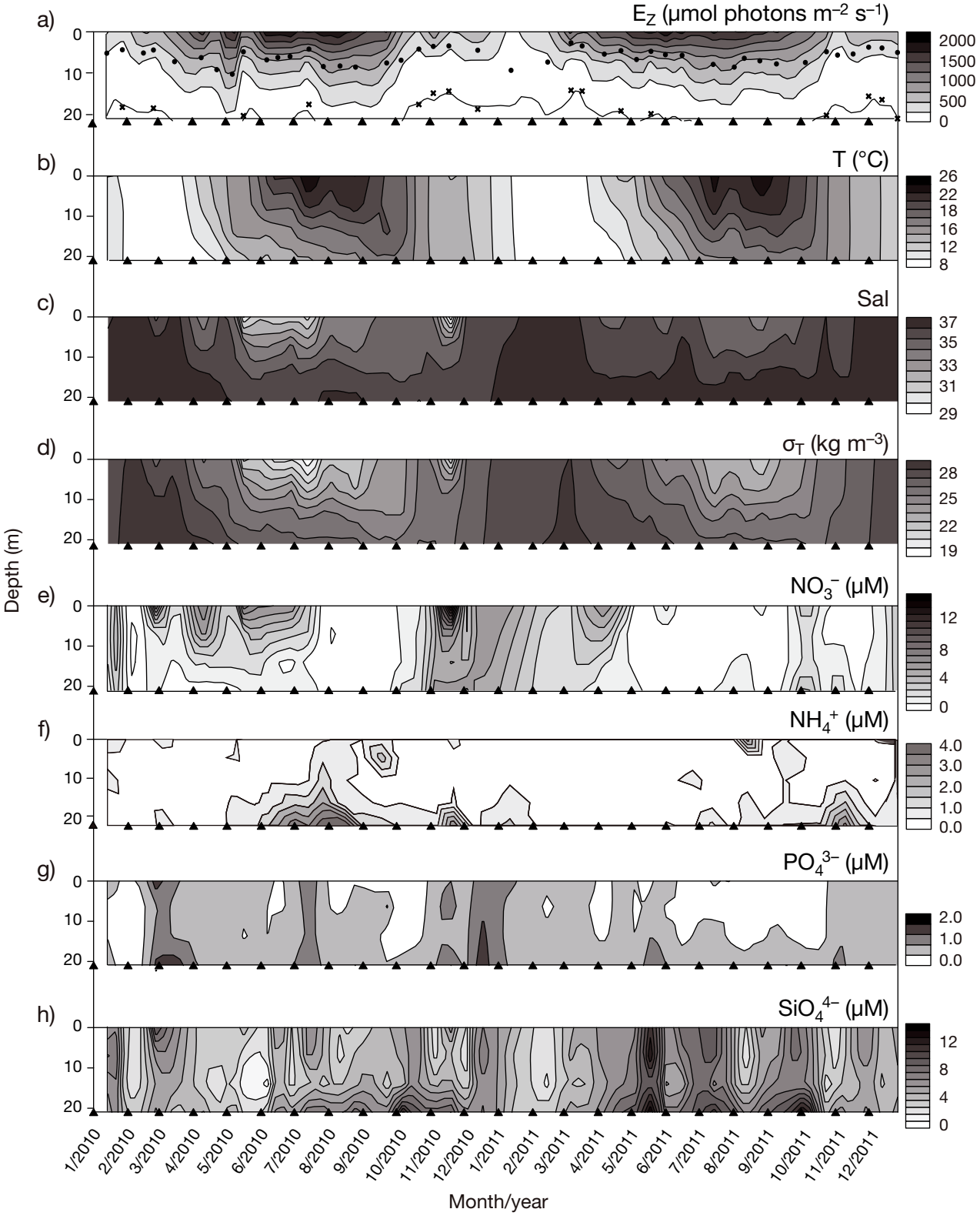

Fig. 2. Physical and chemical properties of the water column. (a) E_z: light intensity in the photosynthetically active ratiation (PAR) spectrum. Dots: calculated first optical depths; crosses: bottom of the euphotic zone (1% light depth), when shallower than the bottom of the water column; (b) temperature (T, °C); (c) salinity (sal); (d) density (σ_T); (e) nitrate; (f) ammonium; (g) phosphate; (h) silicate

bottom (Fig. 2f,g). Surface ammonium peaks were concomitant with high temperatures and high salinity. Higher concentrations of phosphate along the whole water column were only measured in March, July and December 2010, sometimes coinciding with a drop in surface salinity. As with nitrate, annual phosphate concentration in 2011 was lower than in 2010. On the other hand, silicate concentrations were in general higher in 2011 (Fig. 2h). The highest silicate concentrations were measured in summer months of both years in deeper layers and in spring 2011 along the whole water column.

Primary production

Vertical profiles of primary production (PP) showed a decrease with depth (Fig. 3a). The water column maximum i.e. optimal production (P_{opt}) was recorded within the first optical depth, either at 1 m (59% of cases) or 5 m (41%). Generally, when P_{opt} was recorded at 5 m, the difference between PP_{1m} and PP_{5m} was relatively small (<25%). On a few occasions PP showed a more homogenous profile down to 15 m (22 October 2010, 8 March 2011, 18 March 2011, 6 May 2011). PP profiles showed signs of photoinhibition in summer 2011 (2 and 11 August 2011), where PP_{1m} was significantly depressed compared to PP_{5m} (>50% difference). On one occasion (26 August 2010) P_{opt} was recorded at 15 m.

In both 2010 and 2011, P_{opt} was lowest in winter (<1 mg C m^{-3} h^{-1}) and started to increase by the end of April (Fig. 4a). In 2010 P_{opt} increased further and peaked in July (6.54 mg C m^{-3} h^{-1}) and later decreased in the period August–September (<2 mg C m^{-3} h^{-1}). In 2011, however, P_{opt} decreased drastically after the April peak (2.75 mg C m^{-3} h^{-1}), and remained low throughout the May–October period, aside from the peak in late August (3.28 mg C m^{-3} h^{-1}). In both years, autumn peaks were recorded (November 2010: 6.96 mg C m^{-3} h^{-1}; December 2011: 2.74 mg C m^{-3} h^{-1}).

In accordance with the vertical profiles of PP, integrated daily PP (INT PP) showed substantial differences between 2010 and 2011 (Fig. 4a). In 2010 the highest INT PP was calculated for July (565 mg C m^{-2} d^{-1}) concomitantly with high values of incident light (Fig. 2a) and high concentrations of INT chl *a* (38.65 mg m^{-2}; Fig. 4b). In contrast, the highest INT PP of 2011 was reached in October (404 mg C m^{-2} d^{-1}) and did not coincide with the INT chl *a* peak which developed a month later (November: 37.6 mg m^{-2}). These differences resulted in an approximately 1/3 lower estimate of annual PP in 2011 (60.2 g C m^{-2}) as compared to 2010 (87.4 g C m^{-2}).

The seasonal dynamics of P_{opt} and INT PP were relatively closely coupled (Fig. 4a). A stronger decoupling of these parameters occurred in the period May–August 2010, with the exception of the July PP peak, and again in the period from August to the end of October 2011, all of which directly coincided with peaks of P^B_{opt} (Fig. 4c). P^B_{opt} ranged from 0.72–20.84 mg C (mg chl *a*)$^{-1}$ h^{-1}; however, most of the values were constrained to a smaller interval, with a median value of 1.60 mg C (mg chl *a*)$^{-1}$ h^{-1}. Generally, values <5 mg C (mg chl *a*)$^{-1}$ h^{-1} were typical for winter, early spring and late autumn, and higher values were typical for the period June–October.

The product of P_{opt}, the light attenuation coefficient (K_d) and daylight factor (D) explained the majority (85%) of variance in INT PP (Fig. 5a). Chl *a* did not explain a significant portion of variability in P_{opt} (Fig. 5c) in the whole data set. However, in a subset of data (Fig. 5b) comprising diatom dominated assemblages (defined by >60% contribution), chl *a* explained 50% of variability in PP in the surface layer (1 and 5 m).

Phytoplankton biomass and community structure

Phytoplankton community structure expressed as group specific percentage of chl *a* is presented on Fig. 3c–i.

The highest concentrations of chl *a* were found in late autumn of both years (Figs. 3b & 4b), and were associated with a community dominated by diatoms (70–80%, Fig. 3h). Chl *a* reached a maximum of 4.3 mg m^{-3} at 5 m in November 2010 with INT chl *a* of 49.11 mg m^{-2}, and 2.1 mg m^{-3} at 10 m in November 2011 with INT chl *a* of 37.6 mg m^{-2} (Fig. 4b).

A smaller seasonal peak occurred in April and May of both years (1.21–2.01 mg m^{-3}, 20.9–24.6 mg INT chl *a* m^{-2}) and was associated with a community largely composed of prymnesiophytes (up to 60%, Fig. 3g) and diatoms (up to 30%, Fig. 3h) followed by cryptophytes (up to 20%, Fig. 3e) and silicoflagellates (up to 15%, Fig. 3f). A summer peak in biomass was present in July 2010 and was associated with a mixed community of diatoms (up to 80%, Fig. 3h), prymnesiophytes (up to 30%, Fig. 3g) and cyanobacteria (up to 20%, Fig. 3c). Percentage of diatoms and chl *a* concentration increased with depth, reaching 2.99 mg m^{-3} at the bottom. Phytoplankton biomass in the rest of the summer period in 2010 and the whole summer of 2011 was low (<0.6 mg m^{-3}) and dominated by cyanobacteria (up to 35%) and prymnesiophytes (up to 55%).

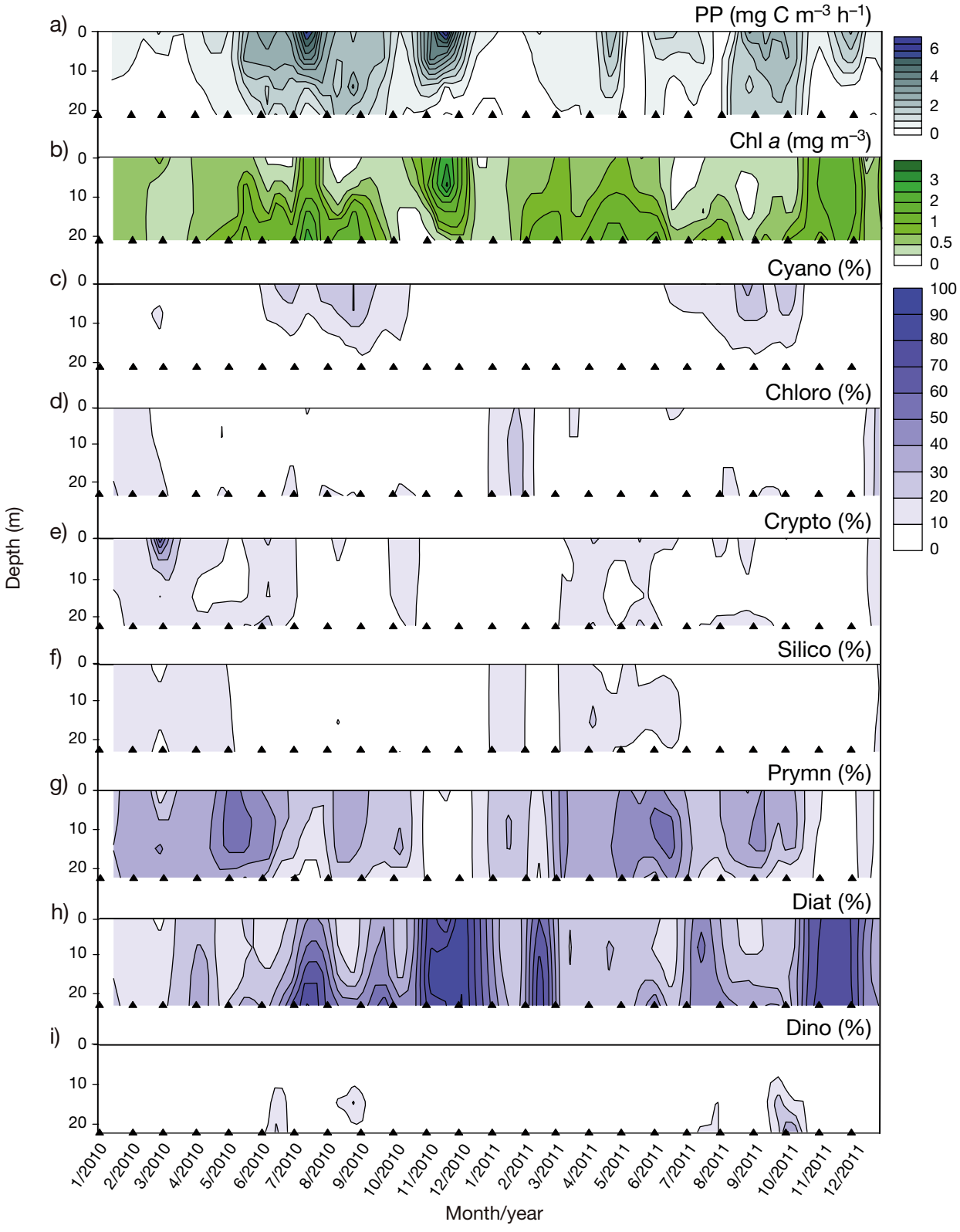

Fig. 3. Water column seasonal dynamics of phytoplankton primary production (PP), biomass and community structure. (a) PP; (b) chl *a* concentration, note the nonlinear scale; (c–i) phytoplankton community structure presented as group-specific percentage of chl *a*. Cyano: cyanobacteria; Chloro: Chlorophytes; Crypto: cryptophytes; Silico: silicoflagellates; Prymn: prymnesiophytes; Diat: diatoms; Dino: dinoflagellates. Note that the colorscale applies to panels c–i

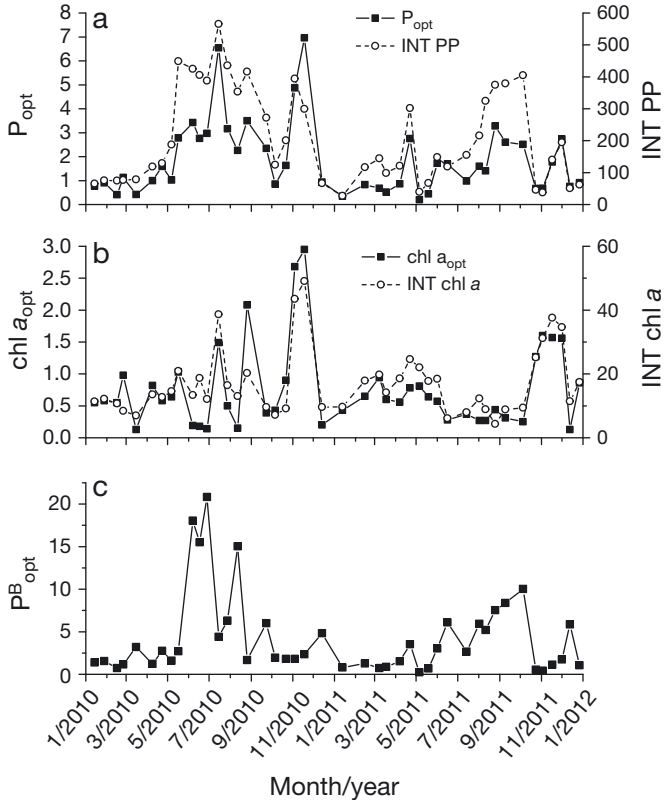

Fig. 4. (a) P_{opt}: water column primary production (PP) maximum (mg C m^{-3} h^{-1}) and INT PP: water column integrated daily PP (mg C m^{-2} d^{-1}); (b) chl a_{opt}: chl *a* concentration at the depth of P_{opt} (mg m^{-3}) and INT chl *a*: water column integrated chl *a* (mg m^{-2}); (c) P^B_{opt}: maximum water column chl *a*-normalized PP (mg C [mg chl *a*]$^{-1}$ h^{-1})

Relationships between environmental factors, phytoplankton production and community structure

Phosphate concentration correlated positively with chl *a* and the percentage of diatoms and negatively with the percentage of prymnesiophytes and cyanobacteria. Nitrate concentration correlated positively with the percentage of cryptophytes and negatively with the percentage of cyanobacteria. Ammonium correlated positively with the percentage dinoflagellates and cyanobacteria and negatively with the percentage of diatoms. Temperature significantly correlated with all abiotic and biotic parameters, except with diatoms and prymnesiophytes. P^B_{opt} correlated positively with cyanobacteria and dinoflagellates and negatively with silicoflagellates and chlorophytes (Table 2).

Aside from silicate, the gradient of all tested abiotic parameters (phosphate, nitrate, ammonium, salinity and temperature) was significantly ($p \leq 0.012$) associated with phytoplankton community structure on the nMDS plot (Fig. 6).

Within the first optical depth (upper 5 m layer), which is relevant for the examination of the relationship between P^B_{opt}, chl *a*, P_{opt} and community structure (Fig. 7a–c), cyanobacteria were associated with the highest values of P^B_{opt} (>5 mg C [mg chl *a*]$^{-1}$ h^{-1}), lowest values of chl *a* (<0.5 mg m^{-3}) and intermediate values of P_{opt} (2–3 mg C m^{-3} h^{-1}). Dinoflagellates were associated with intermediate values of P^B_{opt} (~2 mg C [mg chl *a*]$^{-1}$ h^{-1}), chl *a* (~1 mg m^{-3}) and P_{opt} (~2 mg C m^{-3} h^{-1}). Prymnesiophytes were associated with intermediate values of P^B_{opt} (~3 mg C [mg chl *a*]$^{-1}$ h^{-1}), low values of chl *a* (0.5 mg m^{-3}) and P_{opt} (1–2 mg C m^{-3} h^{-1}). Diatoms were related to the lowest values of P^B_{opt} (<2 mg C [mg chl *a*]$^{-1}$ h^{-1}), and highest values of chl *a* (1–3 mg m^{-3}) and P_{opt} (up to 8 mg C m^{-3} h^{-1}). Communities with a high percentage of chlorophytes and silicoflagellates were associated with low values of P^B_{opt} (1–2 mg C [mg chl *a*]$^{-1}$ h^{-1}), intermediate values of chl *a* (0.5–1 mg m^{-3}) and the lowest values of P_{opt} (~1 mg C m^{-3} h^{-1}).

DISCUSSION

Insights on phytoplankton group-specific primary production

The distribution of P^B_{opt} (water column maximum chl *a*-normalized carbon fixation rate) follows the clustering of phytoplankton groups (Fig. 7, Table 2). Highest values of P^B_{opt} (>5 mg C [mg chl *a*]$^{-1}$ h^{-1}) are typical for phytoplankton communities with a higher percentage of cyanobacteria, in turn associated with high temperature and low nutrients (Fig. 6). Intermediate values (2–3 mg C [mg chl *a*]$^{-1}$ h^{-1}) are typical for phytoplankton communities with a higher percentage of prymnesiophytes, cryptophytes and dinoflagellates. The rest of the phytoplankton groups (diatoms, chlorophytes and silicoflagellates) are associated with lower values of P^B_{opt} (<2 mg C [mg chl *a*]$^{-1}$ h^{-1}) (Fig. 7.), in turn associated with lower temperature and higher nutrient concentration (Fig. 6). With the exception of dinoflagellates, a negative relationship of P^B_{opt} with phytoplankton size was observed, assuming diatoms, chlorophytes and silicoflagellates represent the micro fraction, prymnesiophytes and cryptophytes the nano fraction and cyanobacteria the pico fraction.

In order to compare P^B_{opt} values, obtained from *in situ* data, to the maximal photosynthetic capacity (P^B_{max}) derived from *P-E* experiments, it has to be noted that time-integrated P^B_{opt} is not equivalent to

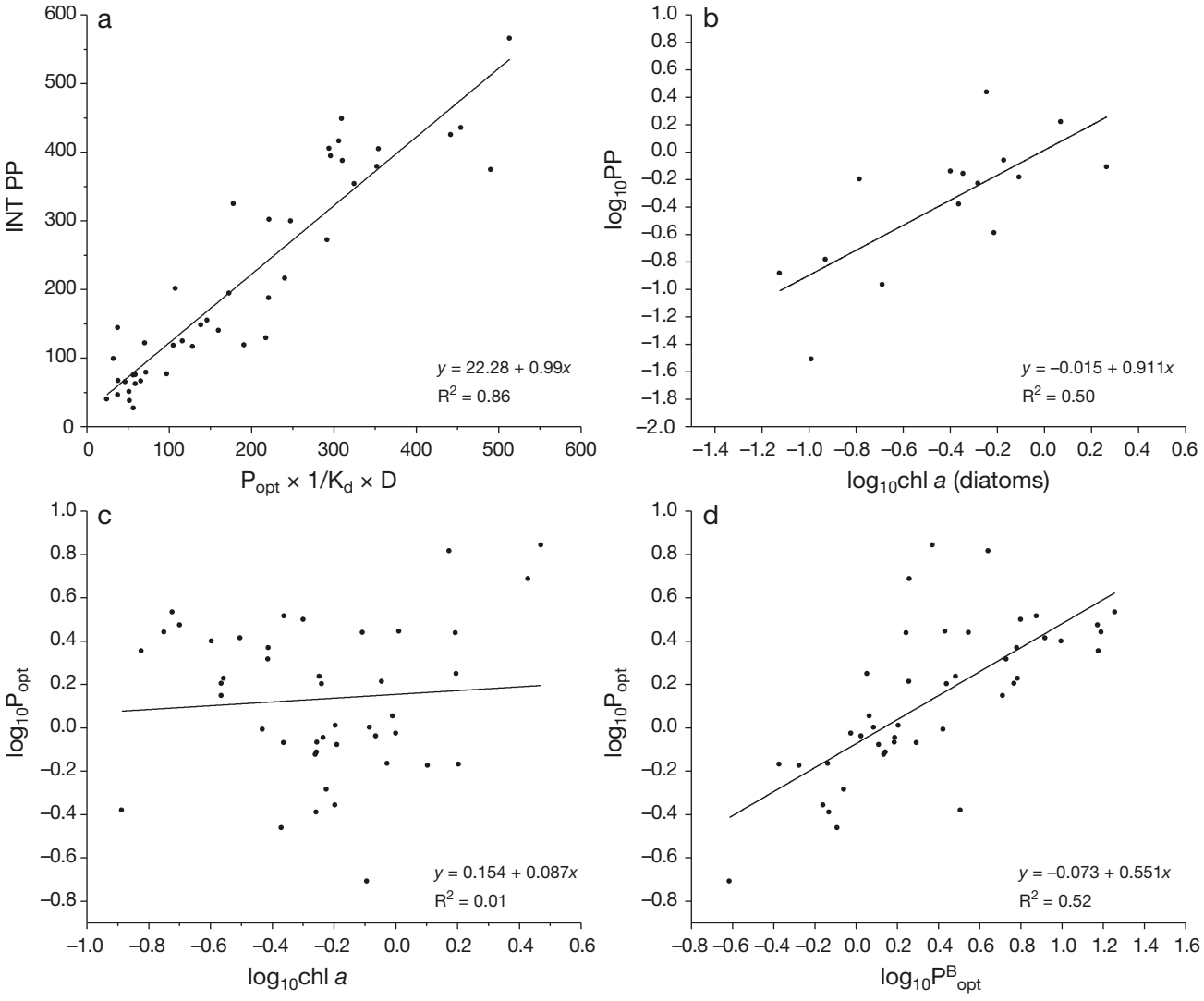

Fig. 5. (a) Empirical model of INT PP (mg C m^{-2} d^{-1}). P_{opt} is the maximum PP of the water column (mg C m^{-3} h^{-1}), K_d is the light attenuation coefficient (m^{-1}) and D is the daylight factor (unitless); (b) linear regression between chl *a* and PP in the first optical depth in a subset of data, where diatoms contributed <60 % to phytoplankton assemblage; (c) linear regression between chl *a* and P_{opt}; (d) linear regression between P^B_{opt} and P_{opt}

time-integrated P^B_{max}, because cells *in situ* can be exposed to sub- or super-saturating irradiance during part of the day (Falkowski & Raven 1997). However, unless photoinhibition is excessive or ambient light is very low, modeling P^B_{opt} is equivalent to modeling near-surface P^B_{max} (Behrenfeld et al. 2002). P^B_{opt} in our data set should correspond to P^B_{max} to a high degree, because photosynthetic rate within the first optical depth was generally light saturated, as indicated by the ratio of *in situ* light to the light saturation index (E_z/E_k > 1, Fig. A1 in the Appendix), and we have omitted the 2 samples from statistical analyses in which photoinhibition was apparent (see 'Materials and methods: Statistical analyses').

The range of P^B_{opt} found in our study is comparable to that of P^B_{max} time series measured in the Bay of Blanes (NW Mediterranean) over 12 yr (Gasol et al. 2016), ranging from 0.5 to 15 mg C (mg chl *a*)$^{-1}$ h^{-1}, where the highest P^B_{max} is reported for the summer months, dominated by cyanobacteria, and the lowest values for the winter months, dominated by microphytoplankton. Gasol et al. (2016) point out the strong positive correlation of P^B_{max} and *Synechoccocus* abundance, but argue that it is probably due to covariation with temperature and stratification, and conclude that community structure plays a minor role in the variability in photophysiology (Gasol et al. 2016). To the contrary, the study of Richardson et al. (2016) high-

Table 2. Spearman's rank correlation matrix for the biological (phytoplankton group-specific percentage of chl *a*, P_{opt}, P^B_{opt}) and the environmental variables (nutrients [PO_4^{3-}, SiO_4^{4+}, NO_3^-, NH_4^+], temperature [T], salinity [sal]) at the first optical depth. dino: dinoflagellates; silico: silicoflagellates; prymn: prymnesiopythes; diat: diatoms; crypto: cryptophytes; cyano: cyanobacteria; chloro: chlorophytes. Statistically significant correlations ($p < 0.05$, $n = 85$) are given in **bold**

	PO_4^{3-}	SiO_4^{4+}	NO_3^-	NH_4^+	P_{opt}	chl *a*	P^B_{opt}	T	sal
PO_4^{3-}	1.00								
SiO_4^{4+}	−0.07	1.00							
NO_3^-	**0.46**	−0.05	1.00						
NH_4^+	−0.02	0.00	0.05						
P_{opt}	0.05	0.00	0.18	0.20	1.00				
chl *a*	**0.33**	−0.08	0.17	−0.17	−0.01	1.00			
P^B_{opt}	**−0.22**	0.09	−0.02	**0.33**	**0.75**	**−0.62**	1.00		
T	**−0.35**	0.03	**−0.37**	**0.30**	**0.55**	**−0.39**	**0.69**	1.00	
sal	0.02	0.04	−0.19	**−0.30**	**−0.64**	**0.27**	**−0.66**	**−0.71**	1.00
% dino	−0.07	−0.19	0.10	**0.29**	**0.41**	0.03	**0.24**	**0.33**	**−0.29**
% silico	−0.01	0.10	0.06	−0.19	**−0.66**	0.06	**−0.52**	**−0.66**	**0.59**
% prymn	**−0.25**	−0.01	−0.08	0.03	−0.13	**−0.34**	0.16	0.05	−0.08
% diat	**0.24**	−0.03	0.01	**−0.23**	0.08	**0.43**	−0.19	−0.02	0.05
% crypto	−0.06	0.19	**0.24**	0.07	**−0.26**	**−0.23**	−0.06	**−0.29**	0.05
% cyano	**−0.42**	0.10	**−0.29**	**0.26**	**0.28**	**−0.62**	**0.62**	**0.64**	**−0.45**
% chloro	0.07	0.00	0.10	0.09	**−0.28**	**0.25**	**−0.36**	**−0.39**	**0.34**

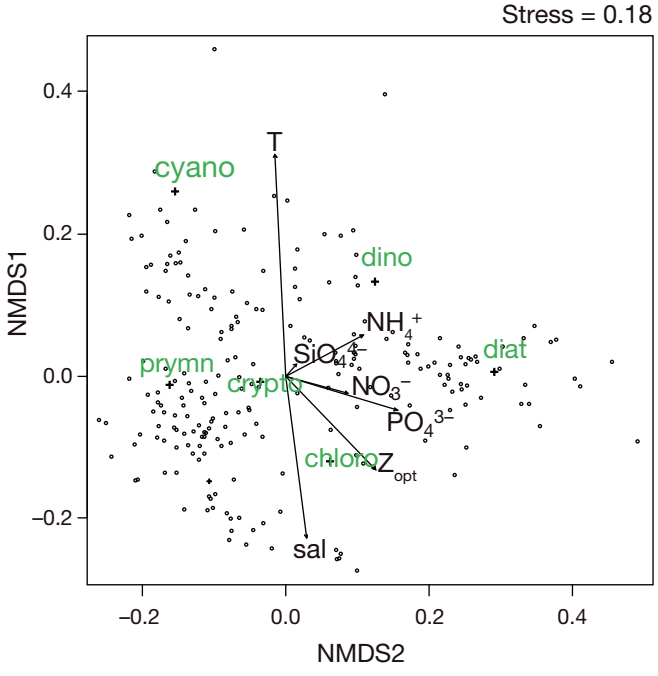

Fig. 6. Non-parametric multidimensional scaling (nMDS) ordination plot showing the relative contribution of phytoplankton groups to community structure (centroids of groups are marked with cross symbols) at all sampling depths (n = 220). Stress = 0.18. Abiotic parameters are represented by arrows and their statistical significance for the community structure indicated by p values in brackets; temperature (T) ($p < 0.001$), salinity (sal) ($p < 0.001$), optical depth (Z_{opt}) ($p < 0.001$), phosphate (PO_4^{3-}) ($p < 0.001$), silicate (SiO_4^{4-}) ($p = 0.791$), ammonium (NH_4^+) ($p = 0.002$) and nitrate (NO_3^-) ($p = 0.012$). See Table 2 for full phytoplankton group names

lights the role of taxon-specific photophysiology in a global data set of photosynthetic parameters. Overall, our results on the relationship of P^B_{opt} and community structure are comparable with the results of Richardson et al. (2016), where high P^B_{max} values were associated with dinoflagellates, small flagellates (prymnesiophytes) and *Synechococcus*, and small P^B_{max} values with diatoms, with the general trend of a negative relationship between P^B_{max} and cell size, as was observed also in our study. The scaling of phytoplankton photosynthesis and cell size has been reported in many studies (Geider et al. 1986, Cermeno et al. 2005, Kameda & Ishizaka 2005, Uitz et al. 2008), however it has been argued that the slope of this relationship is not universal among different phytoplankton taxa, but is assumed to be controlled by the nutrient supply, which determines the community structure across the phytoplankton size spectrum (Marañón 2007). Such a control mechanism is consistent with our results, suggesting that nutrient supply primarily shapes phytoplankton community structure and that the resulting P^B_{opt} is a manifestation of the taxon-specific photophysiology and the relative contribution of different phytoplankton groups to the assemblage.

Nutrients affect PP through changes in phytoplankton community structure

The succession of phytoplankton groups in our study corresponds to the seasonal trends of the nutri-

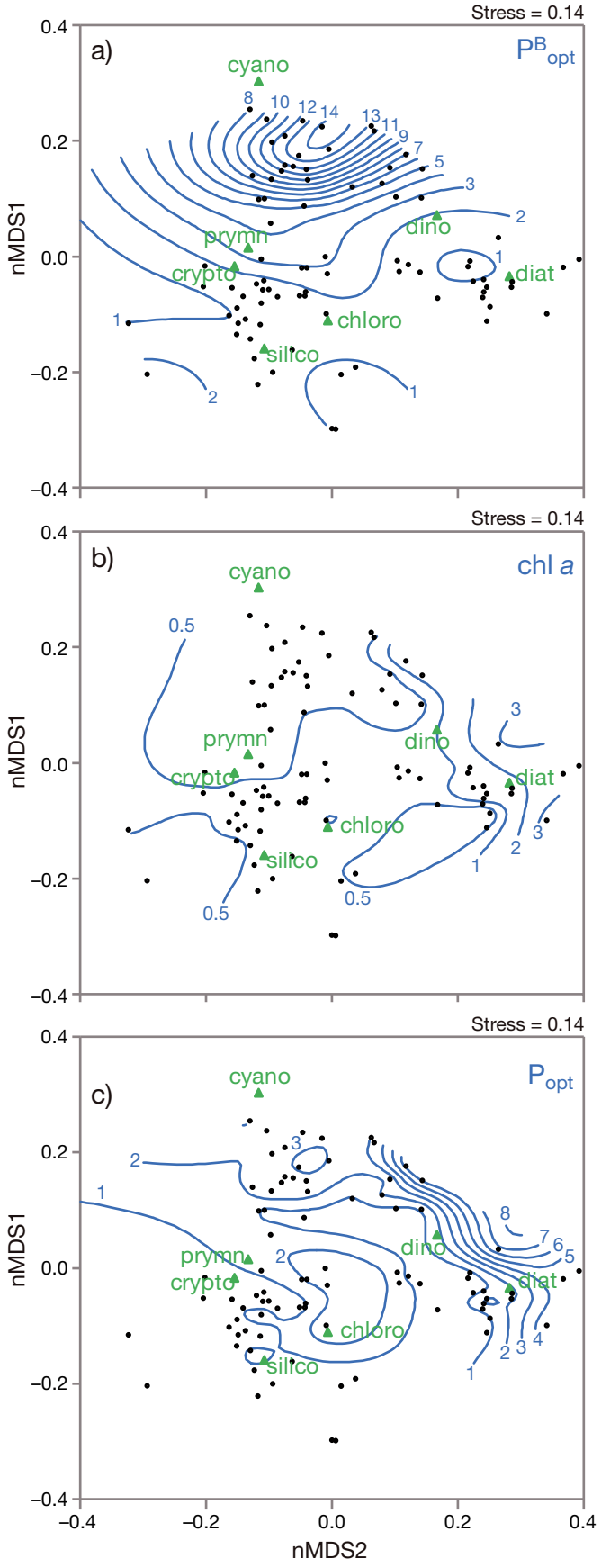

ent, temperature and salinity dynamics (Fig. 6) which are intercorrelated to a high extent (Table 2). As the present study is not supported by adequate methodology to resolve the causality of these correlations, we will not attempt to discuss them in greater detail. Furthermore, we acknowledge the potential effect of other limiting factors on phytoplankton biomass and community composition, including physical advection and the selective grazing pressure on different phytoplankton groups. However, due to the substantial amount of research in the Gulf of Trieste suggesting a dominantly bottom-up controlled freshwater driven system (Mozetič et al. 2012, Vilicic et al. 2013, Cibic et al. 2018), we limit our discussion to the nutrient availability, which is one of the major factors regulating marine productivity and phytoplankton community structure (Regaudie-de-Gioux et al. 2015). In contrast to the PP dynamic (see P_{opt} in Table 2) that was not significantly correlated to nutrient concentration on the interannual scale, the availability of phosphate, ammonium and nitrate was significant for the shaping of the phytoplankton community (Table 2, Fig. 6). We presume that the observed taxonomical clustering in our data is largely due to the size scaling of major parameters of nutrient uptake (Litchman et al. 2007). Smaller cells are in advantage when nutrients are depleted, due to their high surface-area to volume ratio, which reduces the limitation of molecular diffusion during nutrient uptake (Chisholm 1992), and enables them to dominate in nutrient limited conditions (Eppley et al. 1969, Hein & Riemann 1995). Large phytoplankton often dominates when nutrient concentration is high (Tremblay & Legendre 1994, Li 2002). The metabolism of diatoms specifically, is known to react promptly to sudden pulses of nutrient input with extremely high rates of nutrient uptake and cell division (Fawcett & Ward 2011) and may present a crucial advantage of diatoms to outcompete other phytoplankton groups in high (Czerny et al. 2016) and fluctuating (Litchman et al. 2009) nutrient environments, due to diatoms' nutrient storage ability. Accordingly, in our study the gradient of nutrient concentration in the nMDS ordination plot points towards diatoms and away from prymnesio-

Fig. 7. Non-parametric multidimensional scaling (nMDS) ordination plot showing the relative contribution of phytoplankton groups to community structure in the first optical depth (n = 88) (centroids of groups are marked with green triangles). The distribution of biotic parameters in relation to the community structure is delineated by the blue contour lines for (a) P^B_{opt}, (b) chl *a* and (c) P_{opt}. Black dots represent individual samplings. See Table 2 for full phyto-plankton group names

phytes and cyanobacteria (Fig. 6) confirming their competitive success in a high and low nutrient environment, respectively. Typically, low nutrient concentration in the surface layer limits PP during the period of the seasonal irradiance maximum (summer), when cyanobacteria dominate the low biomass phytoplankton assemblage. Aside from being a good nutrient competitor, the dominance of cyanobacteria in the summer surface assemblage can also be due to their high-light adaptation (Moore et al. 1995). On the other hand, nitrate and phosphate enrichment is typically concomitant with an increase in the percentage of diatoms. Phosphate in particular, was found to be significant for the shaping of the community (Fig. 7), with low concentrations significantly correlated to cyanobacteria and prymnesiophytes and high concentrations correlated to diatoms (Table 2). Phosphate is a recognized limiting factor of phytoplankton in the northern Adriatic (Harding et al. 1999, Mozeti et al. 2012) as well as in the eastern (Thingstad et al. 2005) and western Mediterranean (Thingstad et al. 1998). Ammonium was related to dinoflagellates and cyanobacteria, high temperatures and high salinity, implying a greater flow of organic material through the microbial loop during summer and the importance of nitrogen remineralisation in this area in periods of low river flow. The negative correlation of ammonium with diatoms corroborates the view of diatoms being nitrate opportunists (Gilbert et al. 2016).

Minor effect of vertical heterogeneity in the PP profile on INT PP

After accounting for light attenuation (K_d) and the number of hours of daylight (D), an empirical model based on P_{opt} (Fig. 5a) explained the majority of variability in INT PP ($R^2 = 0.86$). Aside from one case (a community with a high percentage of dinoflagellate at 15 m at the end of August 2010, Fig. 3a,i), P_{opt} was always measured in the surface waters, hence a monotonic light-dependent decrease in the vertical profile of PP from the surface maximum can be assumed. However, other instances of decoupling of INT PP and P_{opt} (Fig. 4a) were observed, mostly occurring during the period June–October, due to a greater contribution to INT PP from the deeper layers, suggesting an increase in chl *a*-normalized PP with depth (example October 2011, when dinoflagellates contributed up to 40% of total biomass at 15 m). Decoupling of INT PP and P_{opt} is concomitant with periods when flagellate-dominated phytoplankton communities occurred (prymnesiophytes, cryptophytes and dinoflagellates), and hence the marked vertical differences in photophysiology might be connected to their motility. An active migratory mechanism for maximizing PP has been documented experimentally in the case of dinoflagellates (Ault 2000, Cullen & Horrigan 1981). Additionally, dinoflagellates were associated with the highest light efficiency (photosynthetic parameter α^B) among different phytoplankton taxa in a global study of photosynthetic parameters (Richardson et al. 2016).

Overall, it seems that although the stratified waters in the Gulf of Trieste enable the vertical heterogeneity in biomass and photophysiology, corroborated also by our previous study on phytoplankton photosynthetic parameters (Talaber et al. 2014), this has a minor effect on the estimates of INT PP, because the bulk of INT PP is due to the contribution from the first optical depth. We therefore conclude that measuring PP in the surface is sufficient to adequately estimate daily water column integrated PP in this area during most of the year. Larger discrepancies may only be observed during the summer months, when PP in the surface can be depressed due to photoinhibition processes, arising from the collective effects of high temperature, long exposure to supra-optimal irradiance and nutrient-impoverished conditions at the surface of the stratified water column (Falkowski & Raven 1997). As photoinhibition quickly subsides with depth (Fig. 3a), PP in this period should be measured slightly deeper (i.e. 3–5 m) in the water column, but nevertheless within the first optical depth where light levels are sufficient to saturate photosynthesis (Fig. A1).

Chl *a* is not a good predictor of PP in this coastal site on an interannual scale

Our conclusions with regards to the variability of PP in this area are drived from the measured parameter P_{opt}, since P_{opt} (water column maximum i.e. optimal production) and INT PP (calculated from measurements of all 5 sampling depths) in this data set were tightly coupled (Fig. 4a, Fig. 5a). Chl *a* alone was not recognized as a good predictor of P_{opt} on an interannual scale, as no correlation was found for these 2 biological variables in our data set (Table 2, Fig. 5c). The use of chl *a* as a proxy for phytoplankton PP was recently discredited in another study carried out in a shallow stratified temperate region (Lyngsgaard et al. 2017). Parameter P^B_{opt} on the other hand showed a highly significant positive relationship with P_{opt} in this study (Table 2) and was able to explain

52% of its variability (Fig. 5d), which highlights the importance of community structure for assessing PP in this area. We conclude that when phytoplankton assemblages are diverse, the inclusion of photophysiological parameters is necessary. It follows that chl *a* can only explain a significant portion of PP variability if the community structure is dominated by one phytoplankton group (due to uniform photophysiology, i.e. P^B_{opt}) or rather by one phytoplankton size class, as P^B_{max} / P^B_{opt} is also (negatively) correlated with cell size. This is in line with findings of chl *a* being a good predictor of PP variability in eutrophic coastal environments, where the micro fraction often dominates the phytoplankton assemblage (Margalef 1978, Li 2002), one of the reasons being their ability to escape zooplankton grazing (Irigoien et al. 2005). From our data set we isolated instances when diatoms dominated the asseblage within the first optical depth. Here, chl *a* explained 50% of variability (Fig. 5b). Aside from one winter sampling (February 2011), the rest of this data subset represents samples of the autumn diatom bloom. The autumn bloom is a typical phenomenon of the Gulf of Trieste, although it has significantly decreased in biomass in the last decade, coinciding with a large reduction in average flow rates of the Soča (Isonzo) River and the resulting reduction in nutrient concentrations in the autumn months (Mozetič et al. 2012). Regarding the interannual variability of the autumn diatom bloom specifically, it is safe to conclude that a decrease in biomass signifies a decrease in PP as well.

Estimate of annual PP and the relation to long term phytoplankton trends

In this study, the annual PP was estimated at 87.4 g C m^{-2} and 60.2 g C m^{-2} in 2010 and 2011, respectively, which according to the classification of Nixon (1995) characterizes our sampling site as oligotrophic. Overall, past *in situ* PP estimates for the Adriatic Sea are variable. Annual PP in the Po River plume in the west coast of the northern Adriatic in the 1980s and 1990s was estimated at 150 g C m^{-2} (Revelante & Gilmartin 1983) and 130 g C m^{-2} (Heilmann & Richardson 1999). A much lower estimate of 80 g C m^{-2} was made for an area not under direct river influence on the eastern side of the northern Adriatic (Heilmann & Richardson 1999). Malone et al. (1999) estimated an average PP for the whole North Adriatic of 90 g C m^{-2}. Relative to our estimate for the SE side of the Gulf of Trieste, considerably higher estimates were reported for an area in the Soča (Isonzo) River plume on the NW side by Fonda Umani et al. (2007), ranging 134–414 g C m^{-2} yr^{-1} in the period of 1999–2001. However, in the most recent investigation of primary production in the same part of the Gulf of Trieste (Cibic et al. 2018), the average depth-integrated PP rate during the study period (March 2006–February 2007) was 284 mg C m^{-2} d^{-1}, which translates to roughly 100 g C m^{-2} annually (when multiplied by 356). Cibic et al. (2018) note the decreased PP rates in comparison to older estimates, and relate it to the documented regime shift (Mozeti et al. 2012) in the preceding years. PP estimates in our study are more comparable to a Middle Adriatic coastal site, which is not in the immediate vicinity of a freshwater source, where Grbec et al. (2009) reported a long term (1962–2002) daily average PP of 181 mg C m^{-2}, yielding an annual estimate of about 65 g C m^{-2}.

Diatoms and prymnesiophytes are the dominant groups of the phytoplankton assemblage in the Gulf of Trieste. In the course of this study these groups accounted for the largest percentage of phytoplankton biomass (chl *a*) at any time, aside from shorter periods at the end of summer, when cyanobacteria biomass could reach up to 35% (Fig. 3). Although assemblages associated with a high percentage of cyanobacteria exhibited highest P^B_{opt}, the realized PP was moderate due to extremely low chl *a*. With intermediate P^B_{opt} and low chl *a*, assemblages with a high percentage of prymnesiophytes had even lower rates of PP. The trend of decreasing chl *a* and increasing abundance of nanoflagellates over diatoms (Mozetič et al. 2010, 2012) therefore implies lower PP on an annual scale.

However, isolated fertilization events in summer can significantly increase the annual PP, by creating simultaneously favorable light and nutrient conditions. When a freshening event occurs in the summer period, as happened in July 2010, the nutrient replete conditions make way for a shift in the community towards diatoms and a drastic increase in biomass and PP. Summer diatom blooms in the Gulf of Trieste were reported in the past as rare events (Revelante & Gilmartin 1992), but have been regularly observed in the years after 2005 within a time series that stretches from 1989–2009 (Mozetič et al. 2012). A recurring summer diatom bloom has also been observed off the west coast of the neighboring Istrian peninsula in recent years (Godrijan et al. 2013, Vilicic et al. 2013), that has been directly attributed to the advection of nutrient rich water masses from the Po River delta. Although the influence of the Po River on the Gulf of Trieste is minimal during the prevailing cyclonic geostrophic circulation in the Northern

Adriatic (Artegiani et al. 1997), its influence on the eastern coast of the basin was shown to be important during periods of the Istrian Coastal Countercurrent (Kraus & Supić 2011, Tinta et al. 2015). Whether these changes in the summer phytoplankton assemblage are attributable to the climatic changes in hydrology and/or changes in the circulation dynamics in the North Adriatic, is beyond the scope of this paper. Nevertheless, regardless its origin, a summer nutrient pulse can significantly increase annual PP in this area. Therefore, PP studies in the Gulf of Trieste would greatly benefit from further inspections of the frequency and sources of these summer enrichments.

Acknowledgements. This work was carried out as a part of a PhD thesis at the National Institute of Biology, Slovenia (no. 982/2008) and the research programme 'Coastal Ocean Research' (P1-0237), both financed by the Slovenian Ministry of Higher Education, Science and Technology. We thank Milijan Šiško for his help with statistical analysis and figure preparation. This manuscript has greatly benefited from high quality peer-review.

LITERATURE CITED

Artegiani A, Paschini E, Russo A, Bregant D, Raicich F, Pinardi N (1997) The Adriatic Sea general circulation. II. Baroclinic circulation structure. J Phys Oceanogr 27: 1515–1532

Ault TR (2000) Vertical migration by the marine dinoflagellate *Prorocentrum triestinum* maximises photosynthetic yield. Oecologia 125:466–475

Banse K, Yong M (1990) Sources of variability in satellite derived estimates of phytoplankton production in the eastern tropical Pacific. J Geophys Res Oceans 95: 7201–7215

Barlow RG, Mantoura RFC, Gough MA, Fileman TW (1993) Pigment signatures of the phytoplankton composition in the northeastern Atlantic during the 1990 spring bloom. Deep Sea Res II 40:459–477

Behrenfeld MJ, Falkowski PG (1997) Photosynthetic rates derived from satellite based chlorophyll concentration. Limnol Oceanogr 42:1–20

Behrenfeld MJ, Marañón E, Siegel DA, Hooker SB (2002) Photoacclimation and nutrient-based model of light-saturated photosynthesis for quantifying oceanic primary production. Mar Ecol Prog Ser 228:103–117

Blondeau-Patissier D, Gower JFR, Dekker AG, Phinn SR, Brando VE (2014) A review of ocean color remote sensing methods and statistical techniques for the detection, mapping and analysis of phytoplankton blooms in coastal and open oceans. Prog Oceanogr 123:123–144

Bouman HA, Platt T, Sathyendranath S, Li WKW and others (2003) Temperature as indicator of optical properties and community structure of marine phytoplankton: implications for remote sensing. Mar Ecol Prog Ser 258:19–30

Bouman HA, Nakane T, Oka K, Nakata K, Kurita K, Sathyendranath S, Platt T (2010) Environmental controls on phytoplankton production in coastal ecosystems: a case study from Tokyo Bay. Estuar Coast Shelf Sci 87: 63–72

Bracher A, Bouman HA, Brewin RJW, Bricaud A and others (2017) Obtaining phytoplankton diversity from ocean color: a scientific roadmap for future development. Front Mar Sci 4:55

Cantoni C, Cozzi S, Pecchiar I, Cabrini M, Mozeti P, Catalano G, Fonda Umani S (2003) Short-term variability of primary production and inorganic nitrogen uptake related to the environmental conditions in a shallow coastal area (Gulf of Trieste, N Adriatic Sea). Oceanol Acta 26: 565–575

Cermeño P, Estévez Blanco P, Marañón E, Fernóndez E (2005) Maximum photosynthetic efficiency of size fractionated phytoplankton assessed by ^{14}C uptake and fast repetition rate fluorometry. Limnol Oceanogr 50: 1438–1446

Chisholm SW (1992) Phytoplankton size. In: Falkowsi PG, Woodhead AD (eds) Primary productivity and biogeochemical cycles in the sea. Environ Sci Res, Vol 43. Springer Science & Business Media, New York, NY, p 213–237.

Cibic T, Cerino F, Karuza A, Fornasaro D, Comici C, Cabrini M (2018) Structural and functional response of phytoplankton to reduced river inputs and anomalous physical-chemical conditions in the Gulf of Trieste (northern Adriatic Sea). Sci Total Environ 636:838–853

Claustre H, Babin M, Merien D, Ras J and others (2005) Toward a taxon specific parameterization of bio optical models of primary production: a case study in the North Atlantic. J Geophys Res Oceans 110:C07S12

Cole BE, Cloern JE (1984) Significance of biomass and light availability to phytoplankton productivity in San Francisco Bay. Mar Ecol Prog Ser 17:15–24

Comici C, Bussani A (2007) Analysis of the River Isonzo discharge (1998–2005). Applicata 48:435–454

Cozzi S, Falconi C, Comici C, Čermelj B, Kovac N, Turk V, Giani M (2012) Recent evolution of river discharges in the Gulf of Trieste and their potential response to climate changes and anthropogenic pressure. Estuar Coast Shelf Sci 115:14–24

Cullen JJ, Horrigan SG (1981) Effects of nitrate on the diurnal vertical migration, carbon to nitrogen ratio, and the photosynthetic capacity of the dinoflagellate Gymnodinium splendens. Mar Biol 62:81–89

Czerny JMS, Hauss H, Löscher CR, Riebesell U (2016) Dissolved N:P ratio changes in the eastern tropical North Atlantic: effect on phytoplankton growth and community structure. Mar Ecol Prog Ser 545:49–62

Degobbis D, Gilmartin M (1990) Nitrogen, phosphorus, and biogenic silicon budgets for the northern Adriatic Sea. Oceanol Acta 13:31–45

Dytham C (2011) Choosing and using statistics: a biologist's guide. 3rd edn. Blackwell Science, Malden, MA

Eppley RW, Rogers JN, McCarthy JJ (1969) Half saturation constants for uptake of nitrate and ammonium by marine phytoplankton. Limnol Oceanogr 14:912–920

Everitt DA, Wright SW, Volkman JK, Thomas DP, Lindstrom EJ (1990) Phytoplankton community compositions in the western equatorial Pacific determined from chlorophyll and carotenoid pigment distributions. Deep Sea Res A, Oceanogr Res Pap 37:975–997

Falkowski PG, Raven JA (1997) Aquatic photosynthesis. Blackwell Science, Malden, MA

Fawcett SE, Ward BB (2011) Phytoplankton succession and nitrogen utilization during the development of an upwelling bloom. Mar Ecol Prog Ser 428:13–31

Fonda Umani S, Del Negro P, Larato C, De Vittor C and others (2007) Major inter-annual variations in microbial dynamics in the Gulf of Trieste (northern Adriatic Sea) and their ecosystem implications. Aquat Microb Ecol 46: 163–175

Gallegos CL (2014) Long-term variations in primary production in a eutrophic sub-estuary. I. Seasonal and spatial patterns. Mar Ecol Prog Ser 502:53–67

Gargas E (1975) A manual for phytoplankton primary production studies in the Baltic. Vandkvalitetsinstituttet ATV, Hoersholm

Gasol JM, Cardelús C, Morán XAG, Balagué V and others (2016) Seasonal patterns in phytoplankton photosynthetic parameters and primary production at a coastal NW Mediterranean site. Sci Mar 80 (Suppl 1):63–77

Geider RJ, Platt T, Raven JA (1986) Size dependence of growth and photosynthesis in diatoms: a synthesis. Mar Ecol Prog Ser 30:93–104

Giani M, Djakovac T, Degobbis D, Cozzi S, Solidoro C, Fonda Umani S (2012) Recent changes in the marine ecosystems of the northern Adriatic Sea. Estuar Coast Shelf Sci 115:1–13

Glibert PM, Wilkerson FP, Dugdale RC, Raven JA and others (2016) Pluses and minuses of ammonium and nitrate uptake and assimilation by phytoplankton and implications for productivity and community composition, with emphasis on nitrogen-enriched conditions. Limnol Oceanogr 61:165–197

Godrijan J, Mari D, Tomaži I, Precali R, Pfannkuchen M (2013) Seasonal phytoplankton dynamics in the coastal waters of the north-eastern Adriatic Sea. J Sea Res 77: 32–44

Grasshoff K, Ehrhardt M, Kremling K (1983) Methods of seawater analysis, 2nd edn. Verlag Chemie, Weinheim

Grasshoff K, Ehrhardt M, Kremling K (1999) Methods of seawater analysis, 3rd edn. Wiley-VCH, Weinheim

Grbec B, Morović M, Paklar GB, Kušpilić G, Matijević S, Matić F, Ninčević Gladan Ž (2009) The relationship between the atmospheric variability and productivity in the Adriatic Sea area. J Mar Biol Assoc UK 89:1549–1558

Hager A, Stransky H (1970) The carotenoid pattern and the occurrence of the light-induced xanthophyll cycle in various classes of algae. V. A few members of Cryptophyceae. Arch Mikrobiol 73:77 (in German with English Abstract)

Harding LW, Degobbis D, Precali R (1999) Production and fate of phytoplankton: annual cycles and interannual variability. In: Malone TC, Malej A, Harding LW Jr, Smodlaka N, Turner RE (eds) Ecosystems at the land-sea margin: drainage basin to coastal sea, Vol 55. American Geophysical Union, Washington, DC, p 131–172

Heilmann JP, Richardson K (1999) Phytoplankton distribution and activity in the Northern Adriatic Sea. In: Hopkins TS, Artegiani A, Cauwet G, Degobbis D, Malej A (eds) The Adriatic Sea. Ecosys Research Report No. 32, Proc Workshop 'Physical and biogeochemical processes in the Adriatic Sea', Portonovo (Ancona), Italy, 23–27 April 1996, p 347–362

Hein M, Riemann B (1995) Nutrient limitation of phytoplankton biomass or growth rate: an experimental approach using marine enclosures. J Exp Mar Biol Ecol 188:167–180

Howarth RW (1988) Nutrient limitation of net primary production in marine ecosystems. Annu Rev Ecol Syst 19: 89–110

Iman RL, Conover WJ (1982) A distribution-free approach to inducing rank correlation among input variables. Commun Stat Simul Comput 11:311–334

Irigoien X, Flynn KJ, Harris RP (2005) Phytoplankton blooms: a 'loophole' in microzooplankton grazing impact? J Plankton Res 27:313–321

Kameda T, Ishizaka J (2005) Size-fractionated primary production estimated by a two-phytoplankton community model applicable to ocean color remote sensing. J Oceanogr 61:663–672

Keller AA, Taylor C, Oviatt C, Dorrington T, Holcombe G, Reed L (2001) Phytoplankton production patterns in Massachusetts Bay and the absence of the 1998 winter–spring bloom. Mar Biol 138:1051–1062

Kirk JT (1994) Light and photosynthesis in aquatic ecosystems. Cambridge University Press, Cambridge

Kraus R, Supić N (2011) Impact of circulation on high phytoplankton blooms and fish catch in the northern Adriatic (1990–2004). Estuar Coast Shelf Sci 91: 198–210

Legendre P, Legendre LF (2012) Numerical ecology, Vol 24. Elsevier, Oxford

Li WKW (2002) Macroecological patterns of phytoplankton in the northwestern North Atlantic Ocean. Nature 419: 154–157

Litchman E, Klausmeier CA, Schofield OM, Falkowski PG (2007) The role of functional traits and trade offs in structuring phytoplankton communities: scaling from cellular to ecosystem level. Ecol Lett 10:1170–1181

Litchman E, Klausmeier CA, Yoshiyama K (2009) Contrasting size evolution in marine and freshwater diatoms. Proc Nat Acad Sci 106:2665–2670

Lyngsgaard MM, Markager S, Richardson K, Møller EF, Jakobsen HH (2017) How well does chlorophyll explain the seasonal variation in phytoplankton activity? Estuar Coast 40:1263–1275

Malačič V, Celio M, Čermelj B, Bussani A, Comici C (2006) Interannual evolution of seasonal thermohaline properties in the Gulf of Trieste (northern Adriatic) 1991–2003. J Geophys Res Oceans 111:C08009

Malone TC, Malej A, Harding LW Jr, Smodlaka N, Turner RE (eds) (1999) Ecosystems at the land-sea margin: drainage basin to coastal sea. American Geophysical Union, Washington, DC

Mantoura RFC, Llewellyn CA (1983) The rapid determination of algal chlorophyll and carotenoid pigments and their breakdown products in natural waters by reverse-phase high-performance liquid chromatography. Anal Chim Acta 151:297–314

Marañón E (2007) Inter-specific scaling of phytoplankton production and cell size in the field. J Plankton Res 30: 157–163

Margalef R (1978) Life-forms of phytoplankton as survival alternatives in an unstable environment. Oceanol Acta 1: 493–509

Moore LR, Goericke R, Chisholm SW (1995) Comparative physiology of Synechococcus and Prochlorococcus: influence of light and temperature on growth, pigments, fluorescence and absorptive properties. Mar Ecol Prog Ser 116:259–275

Moreno-Madriñán MJ, Fischer AM (2013) Performance of

the MODIS FLH algorithm in estuarine waters: a multi-year (2003–2010) analysis from Tampa Bay, Florida (USA). Int J Remote Sens 34:6467–6483

Mozetič P, Solidoro C, Cossarini G, Socal G and others (2010) Recent trends towards oligotrophication of the northern Adriatic: evidence from chlorophyll a time series. Estuaries Coasts 33:362–375

Mozetič P, Francé J, Kogovšek T, Talaber I, Malej A (2012) Plankton trends and community changes in a coastal sea (northern Adriatic): bottom-up vs. top-down control in relation to environmental drivers. Estuar Coast Shelf Sci 115:138–148

Murrell MC, Hagy JD, Lores EM, Greene RM (2007) Phytoplankton production and nutrient distributions in a subtropical estuary: importance of freshwater flow. Estuar Coast 30:390–402

Nixon SW (1995) Coastal marine eutrophication: a definition, social causes, and future concerns. Ophelia 41: 199–219

Pugnetti A, Armeni M, Camatti E, Crevatin E and others (2005) Imbalance between phytoplankton production and bacterial carbon demand in relation to mucilage formation in the Northern Adriatic Sea. Sci Total Environ 353:162–177

R Development Core Team (2012) R: a language and environment for statistical computing. R Foundation for Statistical Computing, Vienna www.r-project.org

Regaudie-de-Gioux A, Sal S, López-Urrutia Á (2015) Poor correlation between phytoplankton community growth rates and nutrient concentration in the sea. Biogeosciences 12:1915–1923

Revelante N, Gilmartin M (1983) The phytoplankton of the Adriatic Sea: community structure and characteristics. Thalass Jugosl 19:303–318

Revelante N, Gilmartin M (1992) The lateral advection of particulate organic matter from the Po delta region during summer stratification, and its implications for the northern Adriatic. Estuar Coast Shelf Sci 35:191–212

Richardson K, Bendtsen J, Kragh T, Mousing EA (2016) Constraining the distribution of photosynthetic parameters in the global ocean. Front Mar Sci 3:269

Siegel DA, Doney SC, Yoder JA (2002) The North Atlantic spring phytoplankton bloom and Sverdrup's critical depth hypothesis. Science 296:730–733

Stransky H, Hager A (1970) The carotenoid pattern and the occurrence of the light-induced xanthophyll cycle in various classes of algae. IV. Cyanophyceae and Rhodophyceae. Arch Mikrobiol 72:84–96 (in German with English Abstract)

Strickland JDH, Parsons TR (1968) A practical handbook of seawater analysis. Fish Res Board Can Bull 167:71–75

Talaber I, Francé J, Mozetič P (2014) How phytoplankton physiology and community structure adjust to physical forcing in a coastal ecosystem (northern Adriatic Sea). Phycologia 53:74–85

Terzić S (1996) Biogeochemistry of autochthonous organic matter in neritic areas of the Mediterranean Sea: photosynthetic pigments and carbohydrates. Doctoral dissertation, Faculty of Science, University of Zagreb

Thingstad TF, Zweifel UL, Rassoulzadegan F (1998) P limitation of heterotrophic bacteria and phytoplankton in the northwest Mediterranean. Limnol Oceanogr 43:88–94

Thingstad TF, Krom MD, Mantoura RFC, Flaten GAF and others (2005) Nature of phosphorus limitation in the ultraoligotrophic eastern Mediterranean. Science 309:1068–1071

Tinta T, Vojvoda J, Mozetić P, Talaber I, Vodopivec M, Malfatti F, Turk V (2015) Bacterial community shift is induced by dynamic environmental parameters in a changing coastal ecosystem (northern Adriatic, northeastern Mediterranean Sea)—a 2 year time series study. Environ Microbiol 17:3581–3596

Tremblay JE, Legendre L (1994) A model for the size fractionated biomass and production of marine phytoplankton. Limnol Oceanogr 39:2004–2014

Uitz J, Huot Y, Bruyant F, Babin M, Claustre H (2008) Relating phytoplankton photophysiological properties to community structure on large scales. Limnol Oceanogr 53: 614–630

Uitz J, Claustre H, Gentili B, Stramski D (2010) Phytoplankton class specific primary production in the world's oceans: seasonal and interannual variability from satellite observations. Global Biogeochem Cycles 24:GB3016

Vilicic D, Kuzmic M, Tomažić I, Ljubešić Z and others (2013) Northern Adriatic phytoplankton response to short Po River discharge pulses during summer stratified conditions. Mar Ecol 34:451–466

Wood SN (2003) Thin plate regression splines. J R Stat Soc Series B Stat Methodol 65:95–114

Appendix. Additional data

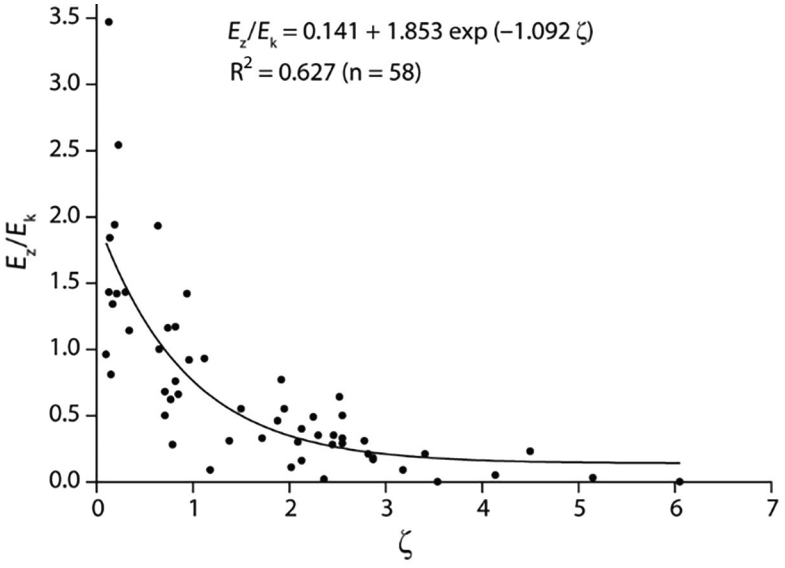

Regression plot of E_z/E_k and optical depth (ζ). The ratio E_z/E_k is an indicator of light limitation (for further details see Talaber et al. 2014). Photosynthesis is light saturated when $E_z/E_k > 1$. E_z: light intensity at depth z (1–21 m); E_k: light saturation index derived from *P-E* experiments (n = 58) carried out in this study area, intermittently in the period May 2009–October 2011, partly covering the period of this study (n = 16)

Editorial responsibility: Katherine Richardson, Copenhagen, Denmark

Submitted: July 18, 2017; Accepted: August 7, 2018
Proofs received from author(s): September 27, 2018